

Duality-Induced Regularizer for Tensor Factorization Based Knowledge Graph Completion

Zhanqiu Zhang Jianyu Cai Jie Wang *

University of Science and Technology of China
 {zzq96, jycai}@mail.ustc.edu.cn, jiewangx@ustc.edu.cn

Abstract

Tensor factorization based models have shown great power in knowledge graph completion (KGC). However, their performance usually suffers from the overfitting problem seriously. This motivates various regularizers—such as the squared Frobenius norm and tensor nuclear norm regularizers—while the limited applicability significantly limits their practical usage. To address this challenge, we propose a novel regularizer—namely, **D**uality-induced **R**egularizer (DURA)—which is not only effective in improving the performance of existing models but widely applicable to various methods. The major novelty of DURA is based on the observation that, for an existing tensor factorization based KGC model (*primal*), there is often another distance based KGC model (*dual*) closely associated with it. Experiments show that DURA yields consistent and significant improvements on benchmarks.

1 Introduction

Knowledge graphs contain quantities of factual triplets, which represent structured human knowledge. In the past few years, knowledge graphs have made great achievements in many areas, such as natural language processing [37], question answering [14], recommendation systems [31], and computer vision [19]. Although commonly used knowledge graphs usually contain billions of triplets, they still suffer from the incompleteness problem that a lot of factual triplets are missing. Due to the large scale of knowledge graphs, it is impractical to find all valid triplets manually. Therefore, knowledge graph completion (KGC)—which aims to predict missing links between entities based on known links automatically—has attracted much attention recently.

Distance based (DB) models and tensor factorization based (TFB) models are two important categories of KGC models. DB models use the Minkowski distance to measure the plausibility of a triplet. Although they can achieve state-of-the-art performance, many of them still have difficulty in modeling complex relation patterns, such as one-to-many and many-to-one relations [17, 33]. TFB models treat knowledge graphs as partially observed third-order binary tensors and formulate KGC as a tensor completion problem. Theoretically, these models are highly expressive and can well handle complex relations. However, their performance usually suffers from the overfitting problem seriously and consequently cannot achieve state-of-the-art.

To tackle the overfitting problem of TFB models, researchers propose various regularizers. The squared Frobenius norm regularizer is a popular one that applies to various models [23, 34, 29]. However, experiments show that it may decrease performance for some models (e.g., RESCAL) [24]. More recently, motivated by the great success of the matrix trace norm in the matrix completion problem [26, 5], Lacroix et al. [16] propose a tensor nuclear p -norm regularizer. It gains significant improvements against the squared Frobenius norm regularizer. However, it is only suitable for canonical polyadic (CP) decomposition [13] based models, such as CP and ComplEx [29], but

*Corresponding author.

not appropriate for a more general class of models, such as RESCAL [23]. Therefore, it is still challenging to find a regularizer that is both widely applicable and effective.

In this paper, we propose a novel regularizer for tensor factorization based KGC models—namely, **D**uality-induced **R**egularizer (DURA). The major novelty of DURA is based on the observation called *duality*—for an existing tensor factorization based KGC model (*primal*), there is often another distance based KGC model closely associated with it (*dual*). The duality can be derived by expanding the squared score functions of the associated distance based models. Then, the cross-term in the expansion is exactly a tensor factorization based KGC model, and the squared terms in it give us a regularizer. Using DURA, we can preserve the expressiveness of tensor factorization based KGC models and prevent them from the overfitting problem. DURA is widely applicable to various tensor factorization based models, including CP, ComplEx, and RESCAL. Experiments show that, DURA yields consistent and significant improvements on datasets for the knowledge graph completion task. It is worth noting that, when incorporated with DURA, RESCAL [23]—which is one of the first knowledge graph completion models—performs comparably to state-of-the-art methods and even beats them on several benchmarks.

2 Preliminaries

In this section, we review the background of this paper in Section 2.1 and introduce the notations used throughout this paper in Section 2.2.

2.1 Background

Knowledge Graph Given a set \mathcal{E} of entities and a set \mathcal{R} of relations, a knowledge graph $\mathcal{K} = \{(e_i, r_j, e_k)\} \subset \mathcal{E} \times \mathcal{R} \times \mathcal{E}$ is a set of triplets, where e_i and r_j are the i -th entity and j -th relation, respectively. Usually, e_i and e_k are also called the head entity and the tail entity, respectively.

Knowledge Graph Completion (KGC) The goal of KGC is to predict valid but unobserved triplets based on the known triplets in \mathcal{K} . KGC models contain two important categories: distance based models and tensor factorization based models, both of which are knowledge graph embedding (KGE) methods. KGE models associate each entity $e_i \in \mathcal{E}$ and relation $r_j \in \mathcal{R}$ with an embedding (may be real or complex vectors, matrices, and tensors) \mathbf{e}_i and \mathbf{r}_j . Generally, they define a score function $s : \mathcal{E} \times \mathcal{R} \times \mathcal{E} \rightarrow \mathbb{R}$ to associate a score $s(e_i, r_j, e_k)$ with each potential triplet $(e_i, r_j, e_k) \in \mathcal{E} \times \mathcal{R} \times \mathcal{E}$. The scores measure the plausibility of triplets. For a query $(e_i, r_j, ?)$, KGE models first fill the blank with each entity in the knowledge graphs and then score the resulted triplets. Valid triplets are expected to have higher scores than invalid triplets.

Distance Based (DB) KGC Models DB models define the score function s with the Minkowski distance. That is, the score functions have the formulation of $s(e_i, r_j, e_k) = -\|\Gamma(e_i, r_j, e_k)\|_p$, where Γ is a model-specific function. Equivalently, we can also use a squared score function $s(e_i, r_j, e_k) = -\|\Gamma(e_i, r_j, e_k)\|_p^2$.

Tensor Factorization Based (TFB) KGC Models TFB models regard a knowledge graph as a third-order binary tensor $\mathcal{X} \in \{0, 1\}^{|\mathcal{E}| \times |\mathcal{R}| \times |\mathcal{E}|}$. The (i, j, k) entry $\mathcal{X}_{ijk} = 1$ if (e_i, r_j, e_k) is valid otherwise $\mathcal{X}_{ijk} = 0$. Suppose that \mathcal{X}_j denotes the j -th frontal slice of \mathcal{X} , i.e., the adjacency matrix of the j -th relation. Usually, a TFB KGC model factorizes \mathcal{X}_j as $\mathcal{X}_j \approx \mathbf{Re}(\bar{\mathbf{H}}\mathbf{R}_j\mathbf{T}^\top)$, where the i -th (k -th) row of \mathbf{H} (\mathbf{T}) is \mathbf{e}_i (\mathbf{e}_k), \mathbf{R}_j is a matrix representing relation r_j , $\mathbf{Re}(\cdot)$ and $\bar{\cdot}$ are the real part and the conjugate of a complex matrix, respectively. That is, the score functions are defined as $s(e_i, r_j, e_k) = \mathbf{Re}(\bar{\mathbf{e}}_i\mathbf{R}_j\mathbf{e}_k^\top)$. Note that the real part and the conjugate of a real matrix are itself. Then, the aim of TFB models is to seek matrices $\mathbf{H}, \mathbf{R}_1, \dots, \mathbf{R}_{|\mathcal{R}|}, \mathbf{T}$, such that $\mathbf{Re}(\bar{\mathbf{H}}\mathbf{R}_j\mathbf{T}^\top)$ can approximate \mathcal{X}_j . Let $\hat{\mathcal{X}}_j = \mathbf{Re}(\bar{\mathbf{H}}\mathbf{R}_j\mathbf{T}^\top)$ and $\hat{\mathcal{X}}$ be a tensor of which the j -th frontal slice is $\hat{\mathcal{X}}_j$. The regularized formulation of a tensor factorization based model can be written as

$$\min_{\hat{\mathcal{X}}_1, \dots, \hat{\mathcal{X}}_{|\mathcal{R}|}} \sum_{j=1}^{|\mathcal{R}|} L(\mathcal{X}_j, \hat{\mathcal{X}}_j) + \lambda g(\hat{\mathcal{X}}), \quad (1)$$

where $\lambda > 0$ is a fixed parameter, $L(\mathcal{X}_j, \hat{\mathcal{X}}_j)$ measures the discrepancy between \mathcal{X}_j and $\hat{\mathcal{X}}_j$, and g is the regularization function.

2.2 Other Notations

We use $h_i \in \mathcal{E}$ and $t_k \in \mathcal{E}$ to distinguish head and tail entities. Let $\|\cdot\|_1$, $\|\cdot\|_2$, and $\|\cdot\|_F$ denote the L_1 norm, the L_2 norm, and the Frobenius norm of matrices or vectors. We use $\langle \cdot, \cdot \rangle$ to represent the inner products of two real or complex vectors. Specifically, if $\mathbf{u}, \mathbf{v} \in \mathbb{C}^{1 \times n}$ are two row vectors in the complex space, then the inner product is defined as $\langle \mathbf{u}, \mathbf{v} \rangle = \bar{\mathbf{u}} \mathbf{v}^\top$.

3 Related Work

Knowledge graph completion (KGC) models include rule-based methods [10, 35], KGE methods, and hybrid methods [11]. This work is related to KGE methods [4, 29, 22, 36]. More specifically, it is related to distance based KGE models and tensor factorization based KGE models.

Distance based models describe relations as relational maps between head and tail entities. Then, they use the Minkowski distance to measure the plausibility of a given triplet. For example, TransE [4] and its variants [33, 17] represent relations as translations in vector spaces. They assume that a valid triplet (h_i, r_j, t_k) satisfies $\mathbf{h}_{i,r_j} + \mathbf{r}_j \approx \mathbf{t}_{k,r_j}$, where \mathbf{h}_{i,r_j} and \mathbf{t}_{k,r_j} mean that entity embeddings may be relation-specific. Structured embedding (SE) [3] uses linear maps to represent relations. Its score function is defined as $s(h_i, r_j, t_k) = -\|\mathbf{R}_j^1 \mathbf{h}_i - \mathbf{R}_j^2 \mathbf{t}_k\|_1$. RotatE [27] defines each relation as a rotation in a complex vector space and the score function is defined as $s(h_i, r_j, t_k) = -\|\mathbf{h}_i \circ \mathbf{r}_j - \mathbf{t}_k\|_1$, where $\mathbf{h}_i, \mathbf{r}_j, \mathbf{t}_k \in \mathbb{C}^k$ and $|\mathbf{r}_j| = 1$. ModE [38] assumes that \mathbf{R}_j^1 is diagonal and \mathbf{R}_j^2 is an identity matrix. It shares a similar score function $s(h_i, r_j, t_k) = -\|\mathbf{h}_i \circ \mathbf{r}_j - \mathbf{t}_k\|_1$ with RotatE but $\mathbf{h}_i, \mathbf{r}_j, \mathbf{t}_k \in \mathbb{R}^k$.

Tensor factorization based models formulate the KGC task as a third-order binary tensor completion problem. RESCAL [23] factorizes the j -th frontal slice of \mathcal{X} as $\mathcal{X}_j \approx \mathbf{A} \mathbf{R}_j \mathbf{A}^\top$, in which embeddings of head and tail entities are from the same space. As the relation specific matrices contain lots of parameters, RESCAL is prone to be overfitting. DistMult [34] simplifies the matrix \mathbf{R}_j in RESCAL to be diagonal, while it sacrifices the expressiveness of models and can only handle symmetric relations. In order to model asymmetric relations, ComplEx [29] extends DistMult to complex embeddings. Both DistMult and ComplEx can be regarded as variants of CP decomposition [13], which are in real and complex vector spaces, respectively.

Tensor factorization based (TFB) KGC models usually suffer from overfitting problem seriously, which motivates various regularizers. In the original papers of TFB models, the authors usually use the squared Frobenius norm (L_2 norm) regularizer [23, 34, 29]. This regularizer cannot bring satisfying improvements. Consequently, TFB models do not gain comparable performance to distance based models [27, 38]. More recently, Lacroix et al. [16] propose to use the tensor nuclear 3-norm [9] (N3) as a regularizer, which brings more significant improvements than the squared Frobenius norm regularizer. However, it is designed for the CP-like models, such as CP and ComplEx, and not suitable for more general models such as RESCAL. Moreover, some regularization methods aim to leverage external background knowledge [20, 7, 21]. For example, to model equivalence and inversion axioms, Minervini et al. [20] impose a set of model-dependent soft constraints on the predicate embeddings. Ding et al. [7] use non-negativity constraints on entity embeddings and approximate entailment constraints on relation embeddings to impose prior beliefs upon the structure of the embeddings space.

4 Methods

In this section, we introduce a novel regularizer—**DU**ality-induced **Regu**larizer (**DURA**)—for tensor factorization based knowledge graph completion. We first introduce basic DURA in Section 4.1 and explain why it is effective in Section 4.2. Then, we introduce DURA in Section 4.3. Finally, we give a theoretical analysis for DURA under some special cases in Section 4.4.

4.1 Basic DURA

Consider the knowledge graph completion problem $(h_i, r_j, ?)$. That is, we are given the head entity and the relation, aiming to predict the tail entity. Suppose that $f_j(i, k)$ measures the plausibility of a

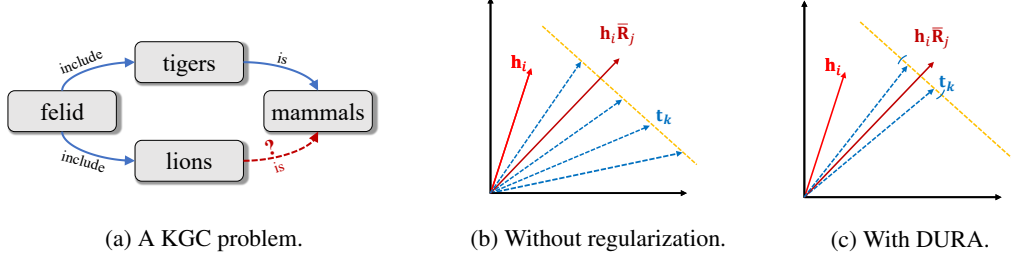


Figure 1: An illustration of why basic DURA can improve the performance of TFB models when the embedding dimensions are 2. Suppose that triplets (h_i, r_j, t_k) ($k = 1, 2, \dots, n$) are valid. (a) Figure 1a demonstrates that tail entities connected to a head entity through the same relation should have similar embeddings. (b) Figure 1b shows that TFB models without regularization can get the same score even though the embeddings of t_k are dissimilar. (c) Figure 1c shows that with DURA, embeddings of t_k are encouraged to locate in a small region.

given triplet (h_i, r_j, t_k) , i.e., $f_j(i, k) = s(h_i, r_j, t_k)$. Then the score function of a TFB model is

$$f_j(i, k) = \text{Re}(\bar{\mathbf{h}}_i \mathbf{R}_j \mathbf{t}_k^\top) = \text{Re}(\langle \mathbf{h}_i \bar{\mathbf{R}}_j, \mathbf{t}_k \rangle). \quad (2)$$

It first maps the entity embeddings \mathbf{h}_i by a linear transformation $\bar{\mathbf{R}}_j$, and then uses the real part of an inner product to measure the similarity between $\mathbf{h}_i \bar{\mathbf{R}}_j$ and \mathbf{t}_k . Notice that another commonly used similarity measure—the squared Euclidean distance—can replace the inner product similarity in Equation (2). We can obtain an associated distance based model formulated as

$$f_j^E(i, k) = -\|\mathbf{h}_i \bar{\mathbf{R}}_j - \mathbf{t}_k\|_2^2. \quad (3)$$

Therefore, there exists a **duality**: for an existing tensor factorization based KGC model (**primal**), there is often another distance based KGC model (**dual**) closely associated with it.

Specifically, the relationship between the primal and the dual can be formulated as

$$\begin{aligned} f_j^E(i, k) &= -\|\mathbf{h}_i \bar{\mathbf{R}}_j - \mathbf{t}_k\|_2^2 \\ &= -\|\mathbf{h}_i \bar{\mathbf{R}}_j\|_2^2 - \|\mathbf{t}_k\|_2^2 + 2\text{Re}(\langle \mathbf{h}_i \bar{\mathbf{R}}_j, \mathbf{t}_k \rangle) \\ &= 2f_j(i, k) - \|\mathbf{h}_i \bar{\mathbf{R}}_j\|_2^2 - \|\mathbf{t}_k\|_2^2. \end{aligned} \quad (4)$$

Usually, we expect $f_j^E(i, k)$ and $f_j(i, k)$ to be higher for all valid triplets (h_i, r_j, t_k) than those for invalid triplets. Suppose that \mathcal{S} is the set that contains all valid triplets. Then, for triplets in \mathcal{S} , we have that

$$\begin{aligned} \max f_j^E(i, k) &= \min -f_j^E(i, k) \\ &= \min -2f_j(i, k) + \|\mathbf{h}_i \bar{\mathbf{R}}_j\|_2^2 + \|\mathbf{t}_k\|_2^2. \end{aligned} \quad (5)$$

By noticing that $\min -2f_j(i, k) = \max 2f_j(i, k)$ is exactly the aim of a TFB model, the duality induces a regularizer for tensor factorization based KGC models, i.e.,

$$\sum_{(h_i, r_j, t_k) \in \mathcal{S}} \|\mathbf{h}_i \bar{\mathbf{R}}_j\|_2^2 + \|\mathbf{t}_k\|_2^2, \quad (6)$$

which is called basic DURA.

4.2 Why Basic DURA Helps

In this section, we demonstrate that basic DURA encourages tail entities connected to a head entity through the same relation to have similar embeddings, which accounts for its effectiveness in improving performance of TFB models.

First, we claim that tail entities connected to a head entity through the same relation should have similar embeddings. Suppose that we know a head entity h_i and a relation r_j , and our aim is to predict the tail entity. If r_j is a one-to-many relation, i.e., there exist two entities t_1 and t_2 such

that both (h_i, r_j, t_1) and (h_i, r_j, t_2) are valid, then we expect that t_1 and t_2 have similar semantics. For example, if two triplets **(felid, include, tigers)** and **(felid, include, lions)** are valid, then **tigers** and **lions** should have similar semantics. Further, we expect that entities with similar semantics have similar embeddings. In this way, if we have known that **(tigers, is, mammals)** is valid, then we can predict that **(lions, is, mammals)** is also valid. See Figure 1a for an illustration of the prediction process.

However, TFB models fail to achieve the above goal. As shown in Figure 1b, suppose that we have known $\mathbf{h}_i \mathbf{R}_j$ when the embedding dimension is 2. Then, we can get the same score $s(h_i, r_j, t_k)$ for $k = 1, 2, \dots, n$ so long as \mathbf{t}_k lies on the same line perpendicular to $\mathbf{h}_i \mathbf{R}_j$. Generally, the entities t_1 and t_2 have similar semantics. However, their embeddings \mathbf{t}_1 and \mathbf{t}_2 can even be orthogonal, which means that the two embeddings are dissimilar. Therefore, the performance of TFB models for knowledge graph completion is usually unsatisfying.

By Equation (5), we know that basic DURA constrains the distance between $\mathbf{h}_i \mathbf{R}_j$ and \mathbf{t}_k . When \mathbf{h}_i and \mathbf{R}_j are known, \mathbf{t}_k lies in a small region (see Figure 1c and we verify this claim in Section 5.4). Therefore, tail entities connected to a head entity through the same relation will have similar embeddings, which is beneficial to the prediction of unknown triplets.

4.3 DURA

Basic DURA encourages tail entities with similar semantics to have similar embeddings. However, it cannot handle the case that head entities have similar semantics.

Suppose that two triplets **(tigers, is, mammals)** and **(lions, is, mammals)** are valid. Similar to the discussion in Section 4.2, we expect that **tigers** and **lions** have similar semantics and thus have similar embeddings. If we further know that **(felid, include, tigers)** is valid, we can predict that **(felid, include, lions)** is valid. However, basic DURA cannot handle the case. Let $\mathbf{h}_1, \mathbf{h}_2, \mathbf{t}_1$, and \mathbf{R}_1 be the embeddings of **tigers, lions, mammals, and is**, respectively. Then, $\mathbf{Re}(\mathbf{h}_1 \mathbf{R}_1 \mathbf{t}_1^\top)$ and $\mathbf{Re}(\mathbf{h}_2 \mathbf{R}_1 \mathbf{t}_1^\top)$ can be equal even if \mathbf{h}_1 and \mathbf{h}_2 are orthogonal, as long as $\mathbf{h}_1 \mathbf{R}_1 = \mathbf{h}_2 \mathbf{R}_1$.

To tackle the above issue, noticing that $\mathbf{Re}(\mathbf{h}_i \mathbf{R}_j \mathbf{t}_k^\top) = \mathbf{Re}(\mathbf{t}_k \mathbf{R}_j^\top \mathbf{h}_i^\top)$, we define another dual distance based KGC model

$$\tilde{f}_j^E(i, k) = -\|\mathbf{t}_k \mathbf{R}_j^\top - \mathbf{h}_i\|_2^2,$$

Then, similar to the derivation in Equation (5), the duality induces a regularizer given by

$$\sum_{(h_i, r_j, t_k) \in \mathcal{S}} \|\mathbf{t}_k \mathbf{R}_j^\top\|^2 + \|\mathbf{h}_i\|^2. \quad (7)$$

When a TFB model are incorporated with regularizer (7), head entities with similar semantics will have similar embeddings.

Finally, combining the regularizer (6) and (7), DURA has the form of

$$\sum_{(h_i, r_j, t_k) \in \mathcal{S}} \left[\|\mathbf{h}_i \mathbf{R}_j\|_2^2 + \|\mathbf{t}_k\|_2^2 + \|\mathbf{t}_k \mathbf{R}_j^\top\|_2^2 + \|\mathbf{h}_i\|_2^2 \right]. \quad (8)$$

4.4 Theoretic Analysis for Diagonal Relation Matrices

If we further relax the summation condition in the regularizer (8) to all possible entities and relations, we can write DURA as:

$$|\mathcal{E}| \sum_{j=1}^{|\mathcal{R}|} (\|\mathbf{H} \mathbf{R}_j\|_F^2 + \|\mathbf{T}\|_F^2 + \|\mathbf{T} \mathbf{R}_j^\top\|_F^2 + \|\mathbf{H}\|_F^2), \quad (9)$$

where $|\mathcal{E}|$ and $|\mathcal{R}|$ are the number of entities and relations, respectively.

In the rest of this section, we use the same definitions of $\hat{\mathcal{X}}_j$ and $\hat{\mathcal{X}}$ as in the problem (1). When the relation embedding matrices \mathbf{R}_j are diagonal in \mathbb{R} or \mathbb{C} as in CP or Complex, the formulation (9) gives an upper bound to the tensor nuclear 2-norm of $\hat{\mathcal{X}}$, which is an extension of trace norm regularizers in matrix completion. To simplify the notations, we take CP as an example, in which all involved embeddings are real. The conclusion in complex space can be analogized accordingly.

Definition 1 (Friedland & Lim [9]). *The nuclear 2-norm of a 3D tensor $\mathcal{A} \in \mathbb{R}^{n_1} \otimes \mathbb{R}^{n_2} \otimes \mathbb{R}^{n_3}$ is*

$$\|\mathcal{A}\|_* = \min \left\{ \sum_{i=1}^r \|\mathbf{u}_{1,i}\|_2 \|\mathbf{u}_{2,i}\|_2 \|\mathbf{u}_{3,i}\|_2 : \mathcal{A} = \sum_{i=1}^r \mathbf{u}_{1,i} \otimes \mathbf{u}_{2,i} \otimes \mathbf{u}_{3,i}, r \in \mathbb{N} \right\},$$

where $\mathbf{u}_{k,i} \in \mathbb{R}^{n_k}$ for $k = 1, \dots, 3$, $i = 1, \dots, r$, and \otimes denotes the outer product.

For notation convenience, we define a relation matrix $\tilde{\mathbf{R}} \in \mathbb{R}^{|\mathcal{R}| \times D}$, of which the j -th row consists of the diagonal entries of \mathbf{R}_j . That is, $\tilde{\mathbf{R}}(j, d) = \mathbf{R}_j(d, d)$, where $\mathbf{R}(i, j)$ represents the entry in the i -th row and j -th column of the matrix \mathbf{R} .

In the knowledge graph completion problem, the tensor nuclear 2-norm of $\hat{\mathcal{X}}$ is

$$\|\hat{\mathcal{X}}\|_* = \min \left\{ \sum_{d=1}^D \|\mathbf{h}_{:d}\|_2 \|\mathbf{r}_{:d}\|_2 \|\mathbf{t}_{:d}\|_2 : \hat{\mathcal{X}} = \sum_{d=1}^D \mathbf{h}_{:d} \otimes \mathbf{r}_{:d} \otimes \mathbf{t}_{:d} \right\},$$

where D is the embedding dimension, $\mathbf{h}_{:d}$, $\mathbf{r}_{:d}$, and $\mathbf{t}_{:d}$ are the d -th columns of \mathbf{H} , $\tilde{\mathbf{R}}$, and \mathbf{T} .

For DURA in (9), we have the following theorem.

Theorem 1. *Suppose that $\hat{\mathcal{X}}_j = \mathbf{H}\mathbf{R}_j\mathbf{T}^\top$ for $j = 1, 2, \dots, |\mathcal{R}|$, where $\mathbf{H}, \mathbf{T}, \mathbf{R}_j$ are real matrices and \mathbf{R}_j is diagonal. Then, the following equation holds*

$$\min_{\hat{\mathcal{X}}_j = \mathbf{H}\mathbf{R}_j\mathbf{T}^\top} \frac{1}{\sqrt{|\mathcal{R}|}} \sum_{j=1}^{|\mathcal{R}|} (\|\mathbf{H}\mathbf{R}_j\|_F^2 + \|\mathbf{T}\|_F^2 + \|\mathbf{T}\mathbf{R}_j^\top\|_F^2 + \|\mathbf{H}\|_F^2) = \|\hat{\mathcal{X}}\|_*.$$

The minimization attains if and only if $\|\mathbf{h}_{:d}\|_2 \|\mathbf{r}_{:d}\|_2 = \sqrt{|\mathcal{R}|} \|\mathbf{t}_{:d}\|_2$ and $\|\mathbf{t}_{:d}\|_2 \|\mathbf{r}_{:d}\|_2 = \sqrt{|\mathcal{R}|} \|\mathbf{h}_{:d}\|_2$, $\forall d \in \{1, 2, \dots, D\}$, where $\mathbf{h}_{:d}$, $\mathbf{r}_{:d}$, and $\mathbf{t}_{:d}$ are the d -th columns of \mathbf{H} , $\tilde{\mathbf{R}}$, and \mathbf{T} , respectively.

Proof. See the supplementary material. □

Therefore, DURA in (9) gives an upper bound to the tensor nuclear 2-norm, which is a tensor analog to the matrix trace norm.

Remark DURA in (8) is actually a weighted version of the one in (9), in which the regularization terms corresponding to the sampled valid triplets. As shown in Srebro & Salakhutdinov [25] and Lacroix et al. [16], the weighted versions of regularizers usually outperform the unweighted regularizer when entries of the matrix or tensor are sampled non-uniformly. Therefore, in the experiments, we implement DURA in a weighted way as in (8).

5 Experiments

In this section, we introduce the experimental settings in Section 5.1 and show the effectiveness of DURA in Section 5.2. We compare DURA to other regularizers in Section 5.3 and visualize the entity embeddings in Section 5.4. Finally, we analyze the sparsity induced by DURA in Section 5.5. The code of HAKE is available on GitHub at <https://github.com/MIRALab-USTC/KGE-DURA>.

5.1 Experimental Settings

We consider three public knowledge graph datasets—WN18RR [28], FB15k-237 [6], and YAGO3-10 [18] for the knowledge graph completion task, which have been divided into training, validation, and testing set in previous works. The statistics of these datasets are shown in Table 1. WN18RR, FB15k-237, and YAGO3-10 are extracted from WN18 [4], FB15k [4], and YAGO3 [18], respectively. Toutanova & Chen [28] and Dettmers et al. [6] indicated the test set leakage problem in WN18 and FB15k, where some

Table 1: Statistics of three benchmark datasets.

	WN18RR	FB15k-237	YAGO3-10
#Entity	40,943	14,541	123,182
#Relation	11	237	37
#Train	86,835	272,115	1,079,040
#Valid	3,034	17,535	5,000
#Test	3,134	20,466	5,000

test triplets may appear in the training dataset in the form of reciprocal relations. They created WN18RR and FB15k-237 to avoid the test set leakage problem, and we use them as the benchmark datasets. We use MRR and Hits@N (H@N) as evaluation metrics. For more details of training and evaluation protocols, please refer to the supplementary material.

Moreover, we find it better to assign different weights for the parts involved with relations. That is, the optimization problem has the form of

$$\min \sum_{(e_i, r_j, e_k) \in \mathcal{S}} [\ell_{ijk}(\mathbf{H}, \mathbf{R}_1, \dots, \mathbf{R}_J, \mathbf{T}) + \lambda(\lambda_1(\|\mathbf{h}_i\|_2^2 + \|\mathbf{t}_k\|_2^2) + \lambda_2(\|\mathbf{h}_i \bar{\mathbf{R}}_j\|_2^2 + \|\mathbf{t}_k \mathbf{R}_j^T\|_2^2))],$$

where $\lambda, \lambda_1, \lambda_2 > 0$ are fixed hyperparameters. We search λ in $\{0.005, 0.01, 0.05, 0.1, 0.5\}$ and λ_1, λ_2 in $\{0.5, 1.0, 1.5, 2.0\}$.

Table 2: Evaluation results on WN18RR, FB15k-237 and YAGO3-10 datasets. We reimplement CP, DistMult, ComplEx, and RESCAL using the “reciprocal” setting [16, 15], which leads to better results than the reported results in the original paper.

	WN18RR			FB15k-237			YAGO3-10		
	MRR	H@1	H@10	MRR	H@1	H@10	MRR	H@1	H@10
RotatE	.476	.428	.571	.338	.241	.533	.495	.402	.670
MuRP	.481	.440	.566	.335	.243	.518	-	-	-
HAKE	.497	.452	.582	.346	.250	.542	.546	.462	.694
Tucker	.470	.443	.526	.358	.266	.544	-	-	-
CP	.438	.414	.485	.333	.247	.508	.567	.494	.698
RESCAL	.455	.419	.493	.353	.264	.528	.566	.490	.701
ComplEx	.460	.428	.522	.346	.256	.525	.573	.500	.703
CP-DURA	.478	.441	.552	.367	.272	.555	.579	.506	.709
RESCAL-DURA	.498	.455	.577	.368	.276	.550	.579	.505	.712
ComplEx-DURA	.491	.449	.571	.371	.276	.560	.584	.511	.713

5.2 Main Results

In this section, we compare the performance of DURA against several state-of-the-art KGC models, including CP [13], RESCAL [23], ComplEx [29], Tucker [2] and some DB models: RotatE [27], MuRP [1], and HAKE [38].

Table 2 shows the effectiveness of DURA. RESCAL-DURA and ComplEx-DURA perform competitively with the SOTA DB models. RESCAL-DURA outperforms all the compared DB models in terms of MRR and H@1. Note that we reimplement CP, ComplEx, and RESCAL under the “reciprocal” setting [15, 16], and obtain better results than the reported performance in the original papers. Overall, TFB models with DURA significantly outperform those without DURA, which shows its effectiveness in preventing models from overfitting.

Generally, models with more parameters and datasets with smaller sizes imply a larger risk of overfitting. Among the three datasets, WN18RR has the smallest size of only 11 kinds of relations and around 80k training samples. Therefore, the improvements brought by DURA on WN18RR are expected to be larger compared with other datasets, which is consistent with the experiments. As stated in Wang et al. [32], RESCAL is a more expressive model, but it is prone to overfit on small- and medium-sized datasets because it represents relations with much more parameters. For example, on WN18RR dataset, RESCAL gets an H@10 score of 0.493, which is lower than ComplEx (0.522). The advantage of its expressiveness does not show up at all. However, incorporated with DURA, RESCAL gets an 8.4% improvement on H@10 and finally attains 0.577, which outperforms all compared models. On larger datasets such as YAGO3-10, overfitting also exists but may be non-significant. Nonetheless, DURA still leads to consistent improvement, demonstrating the ability of DURA to prevent models from overfitting.

Table 3: Comparison between DURA, the squared Frobenius norm (FRO), and the nuclear 3-norm (N3) regularizers. Results of * are taken from Lacroix et al. [16]. CP-N3 and ComplEx-N3 are re-implemented and their performances are better than the reported results in Lacroix et al. [16]. The best performance on each model are marked in bold.

	WN18RR			FB15k-237			YAGO3-10		
	MRR	H@1	H@10	MRR	H@1	H@10	MRR	H@1	H@10
CP-FRO*	.460	-	.480	.340	-	.510	.540	-	.680
CP-N3	.470	.430	.544	.354	.261	.544	.577	.505	.705
CP-DURA	.478	.441	.552	.367	.272	.555	.579	.506	.709
ComplEx-FRO*	.470	-	.540	.350	-	.530	.570	-	.710
ComplEx-N3	.489	.443	.580	.366	.271	.558	.577	.502	.711
ComplEx-DURA	.491	.449	.571	.371	.276	.560	.584	.511	.713
RESCAL-FRO	.397	.363	.452	.323	.235	.501	.474	.392	.628
RESCAL-DURA	.498	.455	.577	.368	.276	.550	.579	.505	.712

5.3 Comparison to Other Regularizers

In this section, we compare DURA to the popular squared Frobenius norm regularizer and the recent tensor nuclear 3-norm (N3) regularizer [16]. The squared Frobenius norm regularizer is given by $g(\hat{\mathcal{X}}) = \|\mathbf{H}\|_F^2 + \|\mathbf{T}\|_F^2 + \sum_{j=1}^{|\mathcal{R}|} \|\mathbf{R}_j\|_F^2$. N3 regularizer is given by $g(\hat{\mathcal{X}}) = \sum_{d=1}^D (\|\mathbf{h}_{:d}\|_3^3 + \|\mathbf{r}_{:d}\|_3^3 + \|\mathbf{t}_{:d}\|_3^3)$, where $\|\cdot\|_3$ denotes L_3 norm of vectors.

We implement both the squared Frobenius norm (FRO) and N3 regularizers in the weighted way as stated in Lacroix et al. [16]. Table 3 shows the performance of the three regularizers on three popular models: CP, ComplEx, and RESCAL. Note that when the TFB model is RESCAL, we only compare DURA to the squared Frobenius norm regularization as N3 does not apply to it.

For CP and ComplEx, DURA brings consistent improvements compared to FRO and N3 on all datasets. Specifically, on FB15k-237, compared to CP-N3, CP-DURA gets an improvement of 0.013 in terms of MRR. Even for the previous state-of-the-art TFB model ComplEx, DURA brings further improvements against the N3 regularizer. Incorporated with FRO, RESCAL performs worse than the vanilla model, which is consistent with the results in Ruffinelli et al. [24]. However, RESCAL-DURA brings significant improvements against RESCAL. All the results demonstrate that DURA is more widely applicable than N3 and more effective than the squared Frobenius norm regularizer.

5.4 Visualization

In this section, we visualize the tail entity embeddings using T-SNE [30] to show that DURA encourages tail entities with similar semantics to have similar embeddings.

Suppose that (h_i, r_j) is a *query*, where h_i and r_j are head entities and relations, respectively. An entity t_k is an *answer* to a query (h_i, r_j) if (h_i, r_j, t_k) is valid. We randomly selected 10 queries in FB15k-237, each of which has more than 50 answers.¹ Then, we use T-SNE to visualize the answers' embeddings generated by CP and CP-DURA. Figure 2 shows the visualization results. Each entity is represented by a 2D point and points in the same color represent tail entities with the same (h_i, r_j) context (i.e. query). Figure 2 shows that, with DURA, entities with the same (h_i, r_j) contexts are indeed being assigned more similar representations, which verifies the claims in Section 4.2.

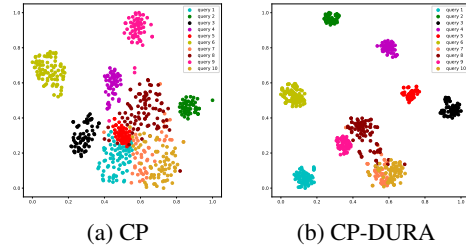


Figure 2: Visualization of the embeddings of tail entities using T-SNE. A point represents a tail entity. Points in the same color represent tail entities that have the same (h_r, r_j) context.

¹For more details about the 10 queries, please refer to the supplementary material.

5.5 Sparsity Analysis

As real-world knowledge graphs usually contain billions of entities, the storage of entity embeddings faces severe challenges. Intuitively, if embeddings are sparse, that is, most of the entries are zero, we can store them with less storage. Therefore, the sparsity of the generated entity embeddings becomes crucial for real-world applications. In this part, we analyze the sparsity of embeddings induced by different regularizers.

Generally, there are few entries of entity embeddings that are exactly equal to 0 after training, which means that it is hard to obtain sparse entity embeddings directly. However, when we score triplets using the trained model, the embedding entries with values close to 0 will have minor contributions to the score of a triplet. If we set the embedding entries close to 0 to be exactly 0, we can transform embeddings into sparse ones. Thus, there is a trade-off between sparsity and performance decrement.

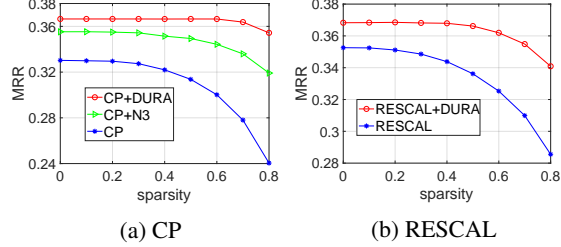


Figure 3: The effect of entity embeddings’ λ -sparsity on MRR. The used dataset is FB15k-237.

We define the following λ -sparsity to indicate the proportion of entries that are close to zero:

$$s_\lambda = \frac{\sum_{i=1}^I \sum_{d=1}^D \mathbb{1}_{\{|x| < \lambda\}}(\mathbf{E}_{id})}{I \times D}, \quad (10)$$

where $\mathbf{E} \in \mathbb{R}^{I \times D}$ is the entity embedding matrix, \mathbf{E}_{id} is the entry in the i -th row and d -th column of \mathbf{E} , I is the number of entities, D is the embedding dimension, and $\mathbb{1}_{\mathcal{C}}(x)$ is the indicator function that takes value of 1 if $x \in \mathcal{C}$ or otherwise the value of 0.

To generate sparse version entity embeddings, following Equation (10), we select all the entries of entity embeddings—of which the absolute value are less than a threshold λ —and set them to be 0. Note that for any given s_λ , we can always find a proper threshold λ to approximate it, as the formula is increasing with respect to λ . Then, we evaluate the quality of sparse version entity embeddings on the knowledge graph completion task. Figure 3 shows the effect of entity embeddings’ λ -sparsity on MRR. Results in the figure show that DURA causes much gentler performance decrement as the embedding sparsity increases. In Figure 3a, incorporated with DURA, CP maintains MRR of 0.366 unchanged even when 60% entries are set to 0. More surprisingly, when the sparsity reaches 70%, CP-DURA can still outperform CP-N3 with zero sparsity. For RESCAL, when setting 80% entries to be 0, RESCAL-DURA still has the MRR of 0.341, which significantly outperforms vanilla RESCAL, whose MRR has decreased from 0.352 to 0.286. In a word, incorporating with DURA regularizer, the performance of CP and RESCAL remains comparable to the state-of-the-art models, even when 70% of entity embeddings’ entries are set to 0.

Following Han et al. [12], we store the sparse version embedding matrices using compressed sparse row (CSR) format or compressed sparse column (CSC) format, which requires $2a + n + 1$ numbers, where a is the number of non-zero elements and n is the number of rows or columns. Experiments show that DURA brings about 65% fewer storage costs for entity embeddings when 70% of the entries are set to 0. Therefore, DURA can significantly reduce the storage usage while maintaining satisfying performance.

6 Conclusion

We propose a widely applicable and effective regularizer—namely, DURA—for tensor factorization based knowledge graph completion models. DURA is based on the observation that, for an existing tensor factorization based KGC model (primal), there is often another distance based KGC model (dual) closely associated with it. Experiments show that DURA brings consistent and significant improvements to TFB models on benchmark datasets. Moreover, visualization results show that DURA can encourage entities with similar semantics to have similar embeddings, which is beneficial to the prediction of unknown triplets.

Appendix

A. Proof for Theorem 1

Theorem 2. Suppose that $\hat{\mathcal{X}}_j = \mathbf{H}\mathbf{R}_j\mathbf{T}^\top$ for $j = 1, 2, \dots, |\mathcal{R}|$, where $\mathbf{H}, \mathbf{T}, \mathbf{R}_j$ are real matrices and \mathbf{R}_j is diagonal. Then, the following equation holds

$$\min_{\hat{\mathcal{X}}_j = \mathbf{H}\mathbf{R}_j\mathbf{T}^\top} \frac{1}{\sqrt{|\mathcal{R}|}} \sum_{j=1}^{|\mathcal{R}|} (\|\mathbf{H}\mathbf{R}_j\|_F^2 + \|\mathbf{T}\|_F^2 + \|\mathbf{T}\mathbf{R}_j^\top\|_F^2 + \|\mathbf{H}\|_F^2) = \|\hat{\mathcal{X}}\|_*.$$

The equation holds if and only if $\|\mathbf{h}_{:d}\|_2\|\mathbf{r}_{:d}\|_2 = \sqrt{|\mathcal{R}|}\|\mathbf{t}_{:d}\|_2$ and $\|\mathbf{t}_{:d}\|_2\|\mathbf{r}_{:d}\|_2 = \sqrt{|\mathcal{R}|}\|\mathbf{h}_{:d}\|_2$, for all $d \in \{1, 2, \dots, D\}$, where $\mathbf{h}_{:d}$, $\mathbf{r}_{:d}$, and $\mathbf{t}_{:d}$ are the d -th columns of \mathbf{H} , \mathbf{R} , and \mathbf{T} , respectively.

Proof. We have that

$$\begin{aligned} & \sum_{j=1}^{|\mathcal{R}|} (\|\mathbf{H}\mathbf{R}_j\|_F^2 + \|\mathbf{T}\|_F^2) \\ &= \sum_{j=1}^{|\mathcal{R}|} \left(\sum_{i=1}^I \|\mathbf{h}_i \circ \mathbf{r}_j\|_F^2 + \sum_{d=1}^D \|\mathbf{t}_{:d}\|_F^2 \right) \\ &= \sum_{j=1}^{|\mathcal{R}|} \left(\sum_{d=1}^D \|\mathbf{t}_{:d}\|_2^2 + \sum_{i=1}^I \sum_{d=1}^D \mathbf{h}_{id}^2 \mathbf{r}_{jd}^2 \right) \\ &= \sum_{j=1}^{|\mathcal{R}|} \sum_{d=1}^D \|\mathbf{t}_{:d}\|_2^2 + \sum_{d=1}^D \|\mathbf{h}_{:d}\|_2^2 \|\mathbf{r}_{:d}\|_2^2 \\ &= \sum_{d=1}^D (\|\mathbf{h}_{:d}\|_2^2 \|\mathbf{r}_{:d}\|_2^2 + |\mathcal{R}| \|\mathbf{t}_{:d}\|_2^2) \\ &\geq \sum_{d=1}^D 2\sqrt{|\mathcal{R}|} \|\mathbf{h}_{:d}\|_2 \|\mathbf{r}_{:d}\|_2 \|\mathbf{t}_{:d}\|_2 \\ &= 2\sqrt{|\mathcal{R}|} \sum_{d=1}^D \|\mathbf{h}_{:d}\|_2 \|\mathbf{r}_{:d}\|_2 \|\mathbf{t}_{:d}\|_2. \end{aligned}$$

The equality holds if and only if $\|\mathbf{h}_{:d}\|_2^2 \|\mathbf{r}_{:d}\|_2^2 = |\mathcal{R}| \|\mathbf{t}_{:d}\|_2^2$, i.e., $\|\mathbf{h}_{:d}\|_2 \|\mathbf{r}_{:d}\|_2 = \sqrt{|\mathcal{R}|} \|\mathbf{t}_{:d}\|_2$.

For all CP decomposition $\hat{\mathcal{X}} = \sum_{d=1}^D \mathbf{h}_{:d} \otimes \mathbf{r}_{:d} \otimes \mathbf{t}_{:d}$, we can always let $\mathbf{h}'_{:d} = \mathbf{h}_{:d}$, $\mathbf{r}'_{:d} = \sqrt{\frac{\|\mathbf{t}_{:d}\|_2 \sqrt{|\mathcal{R}|}}{\|\mathbf{h}_{:d}\|_2 \|\mathbf{r}_{:d}\|_2}} \mathbf{r}_{:d}$ and $\mathbf{t}'_{:d} = \sqrt{\frac{\|\mathbf{h}_{:d}\|_2 \|\mathbf{r}_{:d}\|_2}{\|\mathbf{t}_{:d}\|_2 \sqrt{|\mathcal{R}|}}} \mathbf{t}_{:d}$ such that

$$\|\mathbf{h}'_{:d}\|_2 \|\mathbf{r}'_{:d}\|_2 = \sqrt{|\mathcal{R}|} \|\mathbf{t}'_{:d}\|_2,$$

and meanwhile ensure that $\hat{\mathcal{X}} = \sum_{d=1}^D \mathbf{h}'_{:d} \otimes \mathbf{r}'_{:d} \otimes \mathbf{t}'_{:d}$. Therefore, we know that

$$\begin{aligned} \frac{1}{\sqrt{|\mathcal{R}|}} \sum_{j=1}^{|\mathcal{R}|} \|\hat{\mathcal{X}}_j\|_* &= \frac{1}{2\sqrt{|\mathcal{R}|}} \sum_{j=1}^{|\mathcal{R}|} \min_{\hat{\mathcal{X}}_j = \mathbf{H}\mathbf{R}_j\mathbf{T}^\top} (\|\mathbf{H}\mathbf{R}_j\|_F^2 + \|\mathbf{T}\|_F^2) \\ &\leq \frac{1}{2\sqrt{|\mathcal{R}|}} \min_{\hat{\mathcal{X}}_j = \mathbf{H}\mathbf{R}_j\mathbf{T}^\top} \sum_{j=1}^{|\mathcal{R}|} (\|\mathbf{H}\mathbf{R}_j\|_F^2 + \|\mathbf{T}\|_F^2) \\ &= \min_{\hat{\mathcal{X}} = \sum_{d=1}^D \mathbf{h}_{:d} \otimes \mathbf{r}_{:d} \otimes \mathbf{t}_{:d}} \sum_{d=1}^D \|\mathbf{h}_{:d}\|_2 \|\mathbf{r}_{:d}\|_2 \|\mathbf{t}_{:d}\|_2 \\ &= \|\hat{\mathcal{X}}\|_*. \end{aligned}$$

In the same manner, we know that

$$\frac{1}{2\sqrt{|\mathcal{R}|}} \min_{\hat{\mathcal{X}}_j = \mathbf{H}\mathbf{R}_j\mathbf{T}^\top} \sum_{j=1}^{|\mathcal{R}|} (\|\mathbf{T}\mathbf{R}_j^\top\|_F^2 + \|\mathbf{H}\|_F^2) = \|\hat{\mathcal{X}}\|_*.$$

The equality holds if and only if $\|\mathbf{t}_{:d}\|_2\|\mathbf{r}_{:d}\|_2 = \sqrt{|\mathcal{R}|}\|\mathbf{h}_{:d}\|_2$.

Therefore, the conclusion holds if and only if $\|\mathbf{h}_{:d}\|_2\|\mathbf{r}_{:d}\|_2 = \sqrt{|\mathcal{R}|}\|\mathbf{t}_{:d}\|_2$ and $\|\mathbf{t}_{:d}\|_2\|\mathbf{r}_{:d}\|_2 = \sqrt{|\mathcal{R}|}\|\mathbf{h}_{:d}\|_2, \forall d \in \{1, 2, \dots, D\}$. \square

Therefore, for DURA, we know that

$$\min_{\hat{\mathcal{X}}_j = \mathbf{H}\mathbf{R}_j\mathbf{T}^\top} \frac{1}{\sqrt{|\mathcal{R}|}} g(\hat{\mathcal{X}}) = \|\hat{\mathcal{X}}\|_*,$$

which completes the proof.

Table 4: Comparison to Reg_p1. ‘‘R’’: RESCAL. ‘‘C’’: ComplEx.

	WN18RR			FB15k-237		
	MRR	H@1	H@10	MRR	H@1	H@10
R-Reg_p1	.281	.220	.394	.310	.228	.338
C-Reg_p1	.409	.393	.439	.316	.229	.487
R-DURA	.498	.455	.577	.368	.276	.550
C-DURA	.491	.449	.571	.371	.276	.560

B. The optimal value of p

In DB models, the commonly used p is either 1 or 2. When $p = 2$, DURA takes the form as the one in Equation (8) in the main text. If $p = 1$, we cannot expand the squared score function of the associated DB models as in Equation (4). Thus, the induced regularizer takes the form of $\sum_{(h_i, r_j, t_k) \in \mathcal{S}} \|\mathbf{h}_i \mathbf{R}_j - \mathbf{t}_k\|_1 + \|\mathbf{t}_k \mathbf{R}_j^\top - \mathbf{h}_i\|_1$. The above regularizer with $p = 1$ (Reg_p1) does not gives an upper bound on the tensor nuclear-2 norm as in Theorem 1. Table 4 shows that, DURA significantly outperforms Reg_p1 on WN18RR and FB15k-237. Therefore, we choose $p = 2$.

C. Computational Complexity

Suppose that k is the number of triplets known to be true in the knowledge graph, n is the embedding dimension of entities. Then, for CP and ComplEx, the complexity of DURA is $O(kn)$; for RESCAL, the complexity of DURA is $O(kn^2)$. That is to say, the computational complexity of weighted DURA is the same as the weighted squared Frobenius norm regularizer.

D. More Details About Experiments

In this section, we introduce the training protocol and the evaluation protocol.

D.1 Training Protocol

We adopt the cross entropy loss function for all considered models as suggested in Ruffinelli et al. [24]. We adopt the ‘‘reciprocal’’ setting that creates a new triplet (e_k, r_j^{-1}, e_i) for each triplet (e_i, r_j, e_k) [16, 15]. We use Adagrad [8] as the optimizer, and use grid search to find the best hyperparameters based on the performance on the validation datasets. Specifically, we search learning rates in $\{0.1, 0.01\}$, regularization coefficients in $\{0, 1 \times 10^{-3}, 5 \times 10^{-3}, 1 \times 10^{-2}, 5 \times 10^{-2}, 1 \times 10^{-1}, 5 \times 10^{-1}\}$. On WN18RR and FB15k-237, we search batch sizes in $\{100, 500, 1000\}$ and embedding sizes

Table 5: Hyperparameters found by grid search. k is the embedding size, b is the batch size, λ is the regularization coefficients, and λ_1 and λ_2 are weights for different parts of the regularizer.

	WN18RR					FB15k-237					YAGO3-10				
	k	b	λ	λ_1	λ_2	k	b	λ	λ_1	λ_2	k	b	λ	λ_1	λ_2
CP	2000	100	1e-1	0.5	1.5	2000	100	5e-2	0.5	1.5	1000	1000	5e-3	0.5	1.5
ComplEx	2000	100	1e-1	0.5	1.5	2000	100	5e-2	0.5	1.5	1000	1000	5e-2	0.5	1.5
RESCAL	512	1024	1e-1	1.0	1.0	512	512	1e-1	2.0	1.5	512	1024	5e-2	1.0	1.0

in $\{500, 1000, 2000\}$. On YAGO3-10, we search batch sizes in $\{256, 512, 1024\}$ and embedding sizes in $\{500, 1000\}$. We search both λ_1 and λ_2 in $\{0.5, 1.0, 1.5, 2.0\}$.

We implement DURA in PyTorch and run on all experiments with a single NVIDIA GeForce RTX 2080Ti graphics card.

As we regard the link prediction as a multi-class classification problem and adopt the cross entropy loss, we can assign different weights for different classes (i.e., tail entities) based on their frequency of occurrence in the training dataset. Specifically, suppose that the loss of a given query $(h, r, ?)$ is $\ell((h, r, ?), t)$, where t is the true tail entity, then the weighted loss is

$$w(t)\ell((h, r, ?), t),$$

where

$$w(t) = w_0 \frac{\#t}{\max\{\#t_i : t_i \in \text{training set}\}} + (1 - w_0),$$

w_0 is a fixed number, $\#t$ denotes the frequency of occurrence in the training set of the entity t . For all models on WN18RR and RESCAL on YAGO3-10, we choose $w_0 = 0.1$ and for all the other cases we choose $w_0 = 0$.

We choose a learning rate of 0.1 after grid search. Table 5 shows the other best hyperparameters for DURA found by grid search. Please refer to the Experiments part in the main text for the search range of the hyperparameters.

D.2 Evaluation Protocol

Following Bordes et al. [4], we use entity ranking as the evaluation task. For each triplet (h_i, r_j, t_k) in the test dataset, the model is asked to answer $(h_i, r_j, ?)$ and $(t_k, r_j^{-1}, ?)$. To do this, we fill the positions of missing entities with candidate entities to create a set of candidate triplets, and then rank the triplets in descending order by their scores. Following the ‘‘Filtered’’ setting in Bordes et al. [4], we then filter out all existing triplets known to be true at ranking. We choose Mean Reciprocal Rank (MRR) and Hits at N (H@N) as the evaluation metrics. Higher MRR or H@N indicates better performance. Detailed definitions are as follows.

- The mean reciprocal rank is the average of the reciprocal ranks of results for a sample of queries Q :

$$\text{MRR} = \frac{1}{|Q|} \sum_{i=1}^{|Q|} \frac{1}{\text{rank}_i}.$$

- The Hits@N is the ratio of ranks that no more than N :

$$\text{Hits@N} = \frac{1}{|Q|} \sum_{i=1}^{|Q|} \mathbb{1}_{x \leq N}(\text{rank}_i),$$

where $\mathbb{1}_{x \leq N}(\text{rank}_i) = 1$ if $\text{rank}_i \leq N$ or otherwise $\mathbb{1}_{x \leq N}(\text{rank}_i) = 0$.

D.3 The queries in T-SNE visualization

In Table 6, we list the ten queries used in the T-SNE visualization (Section 5.4 in the main text). Note that a query is represented as $(h, r, ?)$, where h denotes the head entity and r denotes the relation.

Table 6: The queries in T-SNE visualizations.

Index	Query
1	(political drama, /media_common/netflix_genre/titles, ?)
2	(Academy Award for Best Original Song, /award/award_category/winners./award/award_honor/ceremony,?)
3	(Germany, /location/location/contains,?)
4	(doctoral degree, /education/educational_degree/people_with_this_degree./education/education/major_field_of_study,?)
5	(broccoli, /food/food/nutrients./food/nutrition_fact/nutrient,?)
6	(shooting sport, /olympics/olympic_sport/athletes./olympics/olympic_athlete_affiliation/country,?)
7	(synthpop, /music/genre/artists, ?)
8	(Italian American, /people/ethnicity/people,?)
9	(organ, /music/performance_role/track_performances./music/track_contribution/role, ?)
10	(funk, /music/genre/artists, ?)

References

- [1] Balazevic, I., Allen, C., and Hospedales, T. Multi-relational poincaré graph embeddings. In *Advances in Neural Information Processing Systems 32*, pp. 4463–4473, 2019.
- [2] Balazevic, I., Allen, C., and Hospedales, T. TuckER: Tensor factorization for knowledge graph completion. In *Proceedings of the 2019 Conference on Empirical Methods in Natural Language Processing and the 9th International Joint Conference on Natural Language Processing (EMNLP-IJCNLP)*, pp. 5185–5194. Association for Computational Linguistics, 2019.
- [3] Bordes, A., Weston, J., Collobert, R., and Bengio, Y. Learning structured embeddings of knowledge bases. In *Proceedings of the Twenty-Fifth AAAI Conference on Artificial Intelligence*, pp. 301–306. AAAI Press, 2011.
- [4] Bordes, A., Usunier, N., Garcia-Duran, A., Weston, J., and Yakhnenko, O. Translating embeddings for modeling multi-relational data. In *Advances in Neural Information Processing Systems 26*, pp. 2787–2795. Curran Associates, Inc., 2013.
- [5] Candès, E. J. and Recht, B. Exact matrix completion via convex optimization. *Foundations of Computational Mathematics*, 9(6):717, Apr 2009.
- [6] Dettmers, T., Minervini, P., Stenetorp, P., and Riedel, S. Convolutional 2d knowledge graph embeddings. In *Proceedings of the 32th AAAI Conference on Artificial Intelligence*, pp. 1811–1818. AAAI Press, 2018.
- [7] Ding, B., Wang, Q., Wang, B., and Guo, L. Improving knowledge graph embedding using simple constraints. In *Proceedings of the 56th Annual Meeting of the Association for Computational Linguistics (Volume 1: Long Papers)*, pp. 110–121. Association for Computational Linguistics, July 2018.
- [8] Duchi, J., Hazan, E., and Singer, Y. Adaptive subgradient methods for online learning and stochastic optimization. *Journal of Machine Learning Research*, 12(Jul):2121–2159, 2011.
- [9] Friedland, S. and Lim, L.-H. Nuclear norm of higher-order tensors. *Mathematics of Computation*, 87(311):1255–1281, 2018.
- [10] Galárraga, L. A., Teflioudi, C., Hose, K., and Suchanek, F. Amie: Association rule mining under incomplete evidence in ontological knowledge bases. In *Proceedings of the 22nd International Conference on World Wide Web*, pp. 413–422, 2013.
- [11] Guo, S., Wang, Q., Wang, L., Wang, B., and Guo, L. Knowledge graph embedding with iterative guidance from soft rules. In *Proceedings of the Thirty-Second AAAI Conference on Artificial Intelligence*, 2018.
- [12] Han, S., Mao, H., and Dally, W. J. Deep compression: Compressing deep neural network with pruning, trained quantization and huffman coding. In *International Conference on Learning Representations*, 2015.
- [13] Hitchcock, F. L. The expression of a tensor or a polyadic as a sum of products. *Journal of Mathematics and Physics*, 6(1-4):164–189, 1927.

- [14] Huang, X., Zhang, J., Li, D., and Li, P. Knowledge graph embedding based question answering. In *Proceedings of the Twelfth ACM International Conference on Web Search and Data Mining*, pp. 105–113. Association for Computing Machinery, 2019.
- [15] Kazemi, S. M. and Poole, D. Simple embedding for link prediction in knowledge graphs. In *Advances in Neural Information Processing Systems 31*, pp. 4284–4295. Curran Associates, Inc., 2018.
- [16] Lacroix, T., Usunier, N., and Obozinski, G. Canonical tensor decomposition for knowledge base completion. In *Proceedings of the 35th International Conference on Machine Learning*, pp. 2863–2872. PMLR, 2018.
- [17] Lin, Y., Liu, Z., Sun, M., Liu, Y., and Zhu, X. Learning entity and relation embeddings for knowledge graph completion. In *Proceedings of the Twenty-Ninth AAAI Conference on Artificial Intelligence*, pp. 2181–2187. AAAI Press, 2015.
- [18] Mahdisoltani, F., Biega, J., and Suchanek, F. M. YAGO3: A knowledge base from multilingual wikipeas. In *Seventh Biennial Conference on Innovative Data Systems Research*, 2015.
- [19] Marino, K., Salakhutdinov, R., and Gupta, A. The more you know: Using knowledge graphs for image classification. *2017 IEEE Conference on Computer Vision and Pattern Recognition (CVPR)*, pp. 20–28, 2016.
- [20] Minervini, P., Costabello, L., Muñoz, E., Nováček, V., and Vandenbussche, P.-Y. Regularizing knowledge graph embeddings via equivalence and inversion axioms. In Ceci, M., Hollmén, J., Todorovski, L., Vens, C., and Džeroski, S. (eds.), *Machine Learning and Knowledge Discovery in Databases*, pp. 668–683. Springer International Publishing, 2017.
- [21] Minervini, P., Demeester, T., Rocktäschel, T., and Riedel, S. Adversarial sets for regularising neural link predictors. In *Proceedings of the Thirty-Third Conference on Uncertainty in Artificial Intelligence, UAI 2017, Sydney, Australia, August 11-15, 2017*. AUAI Press, 2017.
- [22] Nathani, D., Chauhan, J., Sharma, C., and Kaul, M. Learning attention-based embeddings for relation prediction in knowledge graphs. In *Proceedings of the 57th Annual Meeting of the Association for Computational Linguistics*, pp. 4710–4723, 2019.
- [23] Nickel, M., Tresp, V., and Kriegel, H.-P. A three-way model for collective learning on multi-relational data. In *Proceedings of the 28th International Conference on Machine Learning*, volume 11, pp. 809–816. PMLR, 2011.
- [24] Ruffinelli, D., Broscheit, S., and Gemulla, R. You can teach an old dog new tricks! on training knowledge graph embeddings. In *International Conference on Learning Representations*, 2020.
- [25] Srebro, N. and Salakhutdinov, R. R. Collaborative filtering in a non-uniform world: Learning with the weighted trace norm. In *Advances in Neural Information Processing Systems 23*, pp. 2056–2064. Curran Associates, Inc., 2010.
- [26] Srebro, N., Rennie, J., and Jaakkola, T. S. Maximum-margin matrix factorization. In Saul, L. K., Weiss, Y., and Bottou, L. (eds.), *Advances in Neural Information Processing Systems 17*, pp. 1329–1336. MIT Press, 2005.
- [27] Sun, Z., Deng, Z.-H., Nie, J.-Y., and Tang, J. Rotate: Knowledge graph embedding by relational rotation in complex space. In *International Conference on Learning Representations*, 2019.
- [28] Toutanova, K. and Chen, D. Observed versus latent features for knowledge base and text inference. In *3rd Workshop on Continuous Vector Space Models and Their Compositionality*, 2015.
- [29] Trouillon, T., Welbl, J., Riedel, S., Gaussier, E., and Bouchard, G. Complex embeddings for simple link prediction. In *Proceedings of The 33rd International Conference on Machine Learning*, volume 48, pp. 2071–2080. PMLR, 2016.
- [30] van der Maaten, L. and Hinton, G. Visualizing data using t-SNE. *Journal of Machine Learning Research*, 9:2579–2605, 2008.

- [31] Wang, H., Zhang, F., Wang, J., Zhao, M., Li, W., Xie, X., and Guo, M. Ripplenet: Propagating user preferences on the knowledge graph for recommender systems. In *Proceedings of the 27th ACM International Conference on Information and Knowledge Management*, pp. 417–426. Association for Computing Machinery, 2018.
- [32] Wang, Q., Mao, Z., Wang, B., and Guo, L. Knowledge graph embedding: A survey of approaches and applications. *IEEE Transactions on Knowledge and Data Engineering*, 29(12): 2724–2743, 2017.
- [33] Wang, Z., Zhang, J., Feng, J., and Chen, Z. Knowledge graph embedding by translating on hyperplanes. In *Proceedings of the Twenty-Eighth AAAI Conference on Artificial Intelligence*, pp. 1112–1119. AAAI Press, 2014.
- [34] Yang, B., Yih, S. W.-t., He, X., Gao, J., and Deng, L. Embedding entities and relations for learning and inference in knowledge bases. In *Proceedings of the International Conference on Learning Representations (ICLR) 2015*, 2015.
- [35] Yang, F., Yang, Z., and Cohen, W. W. Differentiable learning of logical rules for knowledge base reasoning. In *Proceedings of the 31st International Conference on Neural Information Processing Systems*, 2017.
- [36] Zhang, S., Tay, Y., Yao, L., and Liu, Q. Quaternion knowledge graph embeddings. In *Advances in Neural Information Processing Systems* 32, pp. 2735–2745, 2019.
- [37] Zhang, Z., Han, X., Liu, Z., Jiang, X., Sun, M., and Liu, Q. ERNIE: Enhanced language representation with informative entities. In *Proceedings of the 57th Annual Meeting of the Association for Computational Linguistics*, pp. 1441–1451. Association for Computational Linguistics, 2019.
- [38] Zhang, Z., Cai, J., Zhang, Y., and Wang, J. Learning hierarchy-aware knowledge graph embeddings for link prediction. In *Proceedings of the Thirty-Fourth AAAI Conference on Artificial Intelligence*. AAAI Press, 2020.